AMERICAN SOCIETY FOR MICROBIOLOGY | Journal of Virology

A Single Amino Acid Substitution in the M Protein Attenuates Japanese Encephalitis Virus in Mammalian Hosts

Mélissanne de Wispelaere,[a]* Cécile Khou,[a] Marie-Pascale Frenkiel,[a] Philippe Desprès,[b] Nathalie Pardigon[a]

Environment and Infectious Risks Unit, Infection and Epidemiology Department, Institut Pasteur, Paris, France[a]; UMR PIMIT (I2T), Université de La Réunion, INSERM U1187, CNRS 9192, IRD 249, Technology Platform CYROI, Saint-Clotilde, La Réunion, France[b]

ABSTRACT

Japanese encephalitis virus (JEV) membrane (M) protein plays important structural roles in the processes of fusion and maturation of progeny virus during cellular infection. The M protein is anchored in the viral membrane, and its ectodomain is composed of a flexible N-terminal loop and a perimembrane helix. In this study, we performed site-directed mutagenesis on residue 36 of JEV M protein and showed that the resulting mutation had little or no effect on the entry process but greatly affected virus assembly in mammalian cells. Interestingly, this mutant virus had a host-dependent phenotype and could develop a wild-type infection in insect cells. Experiments performed on infectious virus as well as in a virus-like particle (VLP) system indicate that the JEV mutant expresses structural proteins but fails to form infectious particles in mammalian cells. Using a mouse model for JEV pathogenesis, we showed that the mutation conferred complete attenuation *in vivo*. The production of JEV neutralizing antibodies in challenged mice was indicative of the immunogenicity of the mutant virus *in vivo*. Together, our results indicate that the introduction of a single mutation in the M protein, while being tolerated in insect cells, strongly impacts JEV infection in mammalian hosts.

IMPORTANCE

JEV is a mosquito-transmitted flavivirus and is a medically important pathogen in Asia. The M protein is thought to be important for accommodating the structural rearrangements undergone by the virion during viral assembly and may play additional roles in the JEV infectious cycle. In the present study, we show that a sole mutation in the M protein impairs the JEV infection cycle in mammalian hosts but not in mosquito cells. This finding highlights differences in flavivirus assembly pathways among hosts. Moreover, infection of mice indicated that the mutant was completely attenuated and triggered a strong immune response to JEV, thus providing new insights for further development of JEV vaccines.

Flaviviruses such as Japanese encephalitis virus (JEV) are arthropod-borne pathogens (arboviruses) that are transmitted through the bite of an infected mosquito and cause serious human diseases worldwide (1). JEV is the causative agent for Japanese encephalitis, one of the most important viral encephalitis diseases of medical interest in Asia, with an incidence of approximately 67,900 human cases per year (2). Up to 30% of the symptomatic cases are fatal, while 30 to 50% of survivors can develop long-term neurologic sequelae (3).

JEV has a positive-sense RNA genome encoding a single polyprotein. This polyprotein is processed by host- and JEV-encoded proteases into 10 proteins: three structural proteins (core [C], premembrane [prM], and envelope [E]) and seven nonstructural (NS) proteins (NS1, NS2A, NS2B, NS3, NS4A, NS4B, and NS5). Like other flaviviruses, JEV enters cells via receptor-mediated endocytosis (4, 5). The acidic environment in the host endosome serves as the physiological trigger for a major conformational change in the E protein that leads to the insertion of its fusion loops in the host endosomal membrane (6, 7). This results in fusion of the viral membrane with the host membrane and delivery of the viral genome to the cytoplasm. The RNA replication occurs within invaginations of the endoplasmic reticulum (ER) (8–10). Following translation, the viral RNA is encapsidated by C to form the nucleocapsid that interacts with the prM and E proteins to bud at the ER membrane. The prM protein acts as a chaperone for proper folding of JEV E protein (11), which leads to the formation of an immature virion. In dengue virus (DV), a related flavivirus, the structure of the immature virus is stabilized through interactions between the prM and E proteins (12–16). The immature flavivirus transits through the secretory pathway, and the decrease in pH induces a rearrangement in the conformation of the membrane proteins that exposes the prM protein furin cleavage site (12, 17). Subsequently, prM is matured by furin into the pr and membrane (M) proteins in the *trans*-Golgi apparatus (12, 17–19). The pr fragment remains in close association with the mature particle until secretion from the cells and prevents premature fusion of viral and cellular membranes within cells (20). The prM cleavage is mandatory to produce infectious particles, since immature particles containing solely uncleaved prM are deficient in membrane fusion (21, 22). Yet, the prM cleavage site is suboptimal, leading to the secretion of partially mature particles (23, 24) that have been shown to interact uniquely with target cells and the

Received 6 May 2015 **Accepted** 30 November 2015

Accepted manuscript posted online 9 December 2015

Citation de Wispelaere M, Khou C, Frenkiel M-P, Desprès P, Pardigon N. 2016. A single amino acid substitution in the M protein attenuates Japanese encephalitis virus in mammalian hosts. J Virol 90:2676–2689. doi:10.1128/JVI.01176-15.

Editor: M. S. Diamond

Address correspondence to Nathalie Pardigon, nathalie.pardigon@pasteur.fr.

* Present address: Mélissanne de Wispelaere, Department of Microbiology and Immunobiology, Harvard Medical School, Boston, Massachusetts, USA.

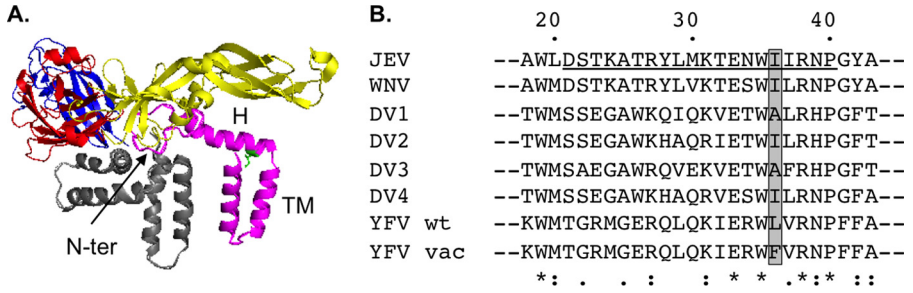

FIG 1 Location of amino acid 36 in JEV M protein. (A) Structure of the E-M mature heterodimer. The structure was derived from the cryoelectron microscopy structure of a mature dengue virus serotype 2 (DV2) (Protein Data Bank [PDB] accession no. 3J27), while the DV2 E protein was replaced with that of Japanese encephalitis virus (JEV) (PDB accession no. 3P54) using PyMOL. Domains I, II, and III of the E protein are colored in red, yellow, and blue, respectively, while E perimembrane and transmembrane helices are colored in gray. The M protein is colored in magenta, each portion being annotated (N-terminal loop [N-ter], perimembrane helix [H], transmembrane helices [TM]), and the isoleucine located at position 36 is colored in green. (B) The sequences for JEV (GenBank accession [GBA] no. AHK05344), West Nile virus (WNV; GBA no. YP_001527877), DV serotypes 1, 2, 3, and 4 (GBA no. U88535, M29095, AY858048, and AY776330, respectively), and yellow fever virus (YFV wild-type [wt] strain, GBA no. AHB63685; and YFV vaccine [vac] strain, GBA no. AGO04419) M perimembrane helices were aligned using ClustalW2. Conserved amino acids (indicated by asterisks) and semiconserved amino acids (indicated by colons and periods) are indicated below the alignment. The perimembrane helix is underlined, and amino acid residue 36, mutagenized in this study, is highlighted in gray.

host immune response (25–29). The prM/M protein thus appears to play important roles in various processes of the viral infection, and further studies are needed to identify the molecular signatures associated with its diverse functions.

The M protein of flaviviruses can be divided into three structurally distinct portions (13, 15): a flexible N-terminal loop (amino acids 1 to 20), an amphipathic perimembrane helix (amino acids 21 to 40), and a pair of transmembrane helices (amino acids 41 to 75) (Fig. 1A). The perimembrane and transmembrane helices serve to anchor the M protein to the membrane. In the case of DV and JEV, the perimembrane helix region was shown to be involved in virus assembly (30–33) and entry (31, 32). Subsequent mutagenesis analysis of the M protein proved the importance of an interactive network between E and M in those processes (16, 34, 35). The flavivirus prM/M protein was also shown to interact with mammalian and mosquito host factors (36–41), thus indicating that this small protein may be involved in additional nonstructural aspects of the flavivirus infectious cycle. Notably, a peptide identified in flavivirus M proteins was shown to potently trigger apoptosis in mammalian cells (42, 43). This proapoptotic phenotype could be alleviated once the residue located at position 36 in the M protein (M-36) of wild-type yellow fever virus (YFV) or DV serotype 2 (DV2), i.e., a leucine or an isoleucine (Fig. 1B), respectively, was mutated to a phenylalanine (42). The residue M-36 lies on the hydrophobic side of the amphipathic helix (Fig. 1), and it is worth noting that phenylalanine, like leucine or isoleucine, is a nonpolar residue and is not expected to modify the nature of the helix. Interestingly, the YFV vaccine strain 17D (YFV-17D) has a phenylalanine at position M-36, which is one of the 32 amino acid differences between YFV-17D and the wild-type YFV Asibi strain from which it was derived (Fig. 1B) (44). While the contribution of this amino acid change to YFV-17D vaccine properties has not been fully evaluated, it is partly responsible for the inability of YFV-17D to infect and disseminate in mosquitoes (45). Additionally, in DV4, the nature of the M-36 residue is crucial for proper viral morphogenesis and subsequent entry, thus highlighting the importance of this residue in various aspects of the flavivirus infectious cycle (32).

In the present study, we examined the impact of a mutation of the isoleucine at position 36 in JEV M into a phenylalanine (M-I36F) on the virus infectious cycle. We show that this sole mutation impairs JEV infection in mammalian cells but not in mosquito cells. By using a virus-like particle system (VLP), we demonstrate that the introduction of the M-I36F mutation impairs assembly and/or secretion of viral particles in mammalian cells. We also show that the JEV(M-I36F) mutant virus is attenuated *in vivo* in a mouse model of JEV infection and that the mice inoculated with the mutant virus produced JEV neutralizing antibodies. Thus, *in vivo* attenuation of JEV can be achieved through the introduction of a single mutation that affects viral assembly/egress, suggesting that such a mutation could be used in the design of efficient new molecular JEV vaccines.

MATERIALS AND METHODS

Cells. *Aedes albopictus* (mosquito) C6/36 cells were maintained at 28°C in Leibovitz medium (L15) supplemented with 10% heat-inactivated fetal bovine serum (FBS). Baby hamster kidney-derived BHK-21, human neuroblastoma-derived SK-N-SH, and human kidney-derived HEK293T cells were maintained at 37°C in Dulbecco modified Eagle medium (DMEM) supplemented with 10% FBS.

Production of recombinant JEV. A molecular cDNA clone of JEV genotype 3 strain RP-9 was kindly provided by Yi-Lin Ling (46). This plasmid was modified as described previously (47). Briefly, the plasmid was first modified to ensure correct propagation in bacteria, through site-directed mutagenesis of a bacterial cryptic promoter located between positions 1787 and 1873 that had not yet been identified in the genome of JEV RP-9 (48). We first used the primer pairs 5′-CAAGCTCAGTGAAGTTGACATCAGGCCACCTG-3′/5′-CAGGTGGCCTGATGTCAACTTCACTGAGCTTG-3′ and 5′-GGCCACCTGAAATGCAGGCTGAAAATGG-3′/5′-CCATTTTCAGCCTGCATTTCAGGTGGCC-3′ to introduce silent mutations predicted to disrupt the bacterial promoter (mutations are underlined), and then we reintroduced a missing nucleotide, A1915, using the primers 5′-AGAAAAATTCTCGTTCGCAAAAAATCCGGCGGACAC-3′ and 5′-GTGTCCGCCGGATTTTTTGCGAACGAGAATTTTTCT-3′. A nonsilent mutation at position 3216, which changed the isoleucine at position 247 in the NS1 protein to a valine, was also reverted to the wild-type sequence using primers 5′-CATCATTCCGCATACCATAGCCGGACCAAAAAGCAA-3′ and 5′-TTGCTTTTTGGTCCGGCTATGGTATGCGGAATGATG-3′. The resulting plasmid, pBR322(CMV)-JEV-RP-9,

could then be stably propagated at 30°C in Stbl2 cells (Life Technologies; catalog no. 10268-019).

The M-I36F mutation was introduced directly in pBR322(CMV)-JEV-RP-9 through PCR mutagenesis using primers 5′-CATGAAAACTGAGAACTGGTTCATAAGGAATCCTGGCTA-3′ and 5′-TAGCCAGGATTCCTTATGAACCAGTTCTCAGTTTTCATG-3′ (the mutation is underlined).

To produce infectious virus, the molecular clones were transfected into C6/36 cells using Lipofectamine 2000 (Life Technologies; catalog no. 11668-019). Once a cytopathic effect was visible, viral supernatants were collected and used as final virus stocks for experiments. The structural part of the JEV(M-I36F) genome was amplified by reverse transcription PCR (RT-PCR) using a SuperScript III One-Step RT-PCR system with Platinum *Taq* DNA polymerase (Life Technologies; catalog no. 12574-018) and the primers 5′-ACGGAAGATAACCATGACTAAAAAACCAGGA-3′ and 5′-TTCTGCAGTCAAGCATGCACATTGGTCGCTAAGA-3′. The PCR fragments were then sequenced by Eurofins Genomics.

Virus infections. For infections, SK-N-SH or C6/36 cells were seeded in 24-well tissue culture plates in DMEM or L15, respectively, supplemented with 2% FBS. Aliquots of virus were diluted in 200 μl of medium and added to the cells. Plates were incubated for 1 h at 37°C or 28°C. Unadsorbed virus was removed by two washes with Dulbecco's phosphate-buffered saline (DPBS), and then 1 ml of DMEM or L15 supplemented with 2% FBS was added to the cells, followed by incubation at 37°C or 28°C until collection.

Recombinant virus transfections. For transfections, HEK293T cells were seeded in 24-well tissue culture plates in DMEM supplemented with 2% FBS. Transfections were performed using Lipofectamine 2000 (Life Technologies; catalog no. 11668-019) according to the manufacturer's instructions. The cells were incubated at 37°C until collection.

Antibodies. Mouse hybridomas producing the monoclonal antibody 4G2 anti-flavivirus E were purchased from the ATCC (catalog no. HB-112), and a highly purified antibody preparation was produced by RD Biotech (Besançon, France). Rabbit polyclonal antibody anti-JEV C was kindly provided by Yoshiharu Matsuura (49). Rabbit polyclonal antibody anti-JEV M was kindly provided by Young-Min Lee (50). The antibody against prM was obtained by collecting sera from mice immunized against JEV-RP-9. The antibodies against calnexin and actin were purchased from Enzo Life Sciences (catalog no. ADI-SPA-865) and Abnova (catalog no. MAB8172), respectively. Horseradish peroxidase (HRP)-conjugated goat anti-mouse and anti-rabbit IgG antibodies were obtained from Bio-Rad Laboratories (catalog no. 170-6516 and 170-6515, respectively). Alexa Fluor 488-conjugated goat anti-mouse IgG antibody was obtained from Jackson ImmunoResearch (catalog no. 115-545-003).

Focus-forming assay (FFA). BHK-21 or C6/36 cells were seeded in 24-well plates. Tenfold dilutions of virus samples were prepared in duplicate in DMEM (BHK-21) or L15 (C6/36), and 200 μl of each dilution was added to the cells. The plates were incubated for 1 h at 37°C (BHK-21) or 28°C (C6/36). Unadsorbed virus was removed, after which 1 ml of DMEM (BHK-21) or L15 (C6/36) supplemented with 1.6% carboxymethyl cellulose (CMC), 10 mM HEPES buffer, 72 mM sodium bicarbonate, and 2% FBS was added to each well, followed by incubation at 37°C for 32 h (BHK-21) or at 28°C for 54 h (C6/36). The CMC overlay was aspirated, and the cells were washed with PBS and fixed with 4% paraformaldehyde for 15 min, followed by permeabilization with 0.1% Triton X-100 for 5 min. After fixation, the cells were washed with PBS and incubated for 1 h at room temperature with anti-E antibody (4G2), followed by incubation with HRP-conjugated anti-mouse IgG antibody. The assays were developed with the Vector VIP peroxidase substrate kit (Vector Laboratories; catalog no. SK-4600) according to the manufacturer's instructions. The viral titers were expressed in focus-forming units (FFU) per milliliter.

Western blotting. Protein lysates were prepared by cell lysis in radioimmunoprecipitation assay (RIPA) buffer (Bio Basic; catalog no. RB4476) containing protease inhibitors (Roche; catalog no. 11873580001). Equal amounts of proteins, supernatants, or purified VLPs were loaded on a NuPAGE Novex 4 to 12% Bis-Tris protein gel (Life Technologies) and transferred to a polyvinylidene difluoride (PVDF) membrane (Bio-Rad; catalog no. 170-4156) by use of the Trans-Blot Turbo transfer system (Bio-Rad). After the membrane was blocked for 1 h at room temperature in PBS-Tween (PBS-T) plus 5% milk, the blot was incubated overnight at 4°C with appropriate dilutions of the primary antibodies. The membrane was then washed in PBS-T and then incubated for 1 h at room temperature in the presence of HRP-conjugated secondary antibodies. After washes in PBS-T, the membrane was developed using a Pierce ECL Western blotting substrate (Thermo Scientific; catalog no. 32106) and exposed to film. When necessary, the bands were quantified using ImageJ (W. S. Rasband, U.S. National Institutes of Health, Bethesda, MD; http://imagej.nih.gov/ij/; 1997-2015).

Coimmunoprecipitation. Coimmunoprecipitations were performed using a Pierce coimmunoprecipitation kit (26149; Thermo Fisher Scientific) according to the manufacturer's instructions. Agarose beads were incubated with 60 μg of anti-E antibody (4G2) for 2 h at room temperature under constant rocking. Infected BHK-21 cells were lysed in the manufacturer's lysis buffer, and 12 μg of cell lysates was then incubated with agarose beads coupled with 4G2 antibody overnight at 4°C. The beads were then washed, and the captured protein complexes were eluted, in accordance with the manufacturer's instructions. Twenty-microliter volumes of eluates were then analyzed by Western blotting.

Endo-H assay. Equal amounts of protein lysates were subjected to digestion with endo-β-*N*-acetylglucosaminidase H (endo-H) (P0702S; New England BioLabs) in the presence of the manufacturer's buffer G5 and protease inhibitors (11836170001; Roche) for 30 min at 37°C. Undigested and digested samples were separated on an 8% Tris-glycine polyacrylamide gel and then analyzed by Western blotting as described above.

Quantitative RT-PCR (RT-qPCR). RNA was extracted from samples using NucleoSpin RNA (Macherey-Nagel; catalog no. 740955) according to the manufacturer's instructions.

The RNA standard used for quantification of JEV copy numbers was an *in vitro* transcript synthesized from a ClaI-linearized JEV-RP-9 replicon plasmid, J-R2A (51). *In vitro* transcripts were synthesized using a MEGAscript SP6 transcription kit (Life Technologies; catalog no. AM1330) in accordance with the manufacturers' instructions, and the absence of template DNA after DNase digestion was monitored through the absence of qPCR amplification from the *in vitro* transcript.

The quantitation of a given target RNA was done on 8 μl or 200 ng of RNA using the QuantiTect SYBR green RT-PCR kit (Qiagen; catalog no. 204243) according to the manufacturer's instructions. The MiniOpticon real-time PCR system (Bio-Rad) was used to measure SYBR green fluorescence with the following program: reverse transcription step at 50°C (30 min), followed by an initial PCR activation step at 95°C (15 min), 40 cycles of denaturation at 94°C (15 s), annealing at 60°C (30 s), and extension at 72°C (30 s). Results were analyzed using the CFX Manager software (Bio-Rad). Primers 5′-GCCGGGTGGGACACTAGAAT-3′ and 5′-TGGACAGCGATGTTCGTGAA-3′ were used for viral genome quantification (52). Target gene expression was normalized to the expression of actin mRNA, measured using the primers 5′-GTACCACTGGCATCGTGATGGACT-3′ and 5′-CCGCTCATTGCCAATGGTGAT-3′.

Immunofluorescence analysis (IFA). Cells were grown on coverslips and fixed with methanol for 15 min at −20°C. After fixation, the cells were washed with PBS, and JEV proteins were detected with appropriate dilutions of the primary antibodies, followed by incubation with fluorophore-conjugated secondary antibodies. The coverslips were mounted with ProLong gold antifade reagent with DAPI (Life Technologies; catalog no. P36931). The slides were examined using a fluorescence microscope (Axioplan 2 Imaging; Zeiss).

Virus-like particle (VLP) production. The fragment encompassing the prM and E structural genes of JEV-RP-9 was amplified using the primers 5′-TTGTCGACATGGGAGGAAATGAAGGCT-3′ (SalI site underlined) and 5′-TTCTGCAGTCAAGCATGCACATTGGTCGCTAAGA-3′ (PstI site underlined). The fragment was digested with SalI and PstI

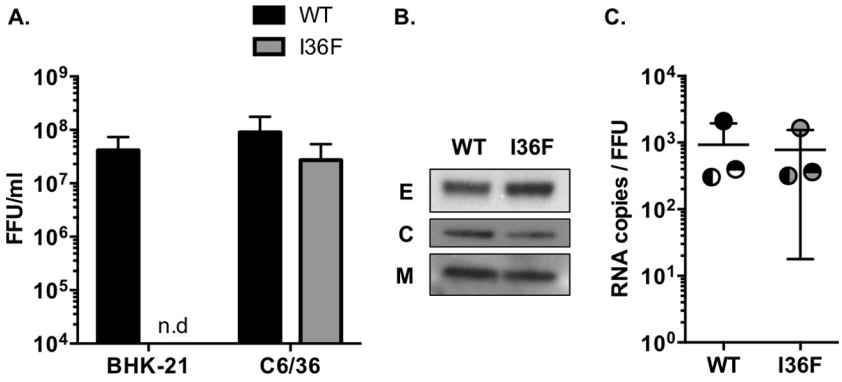

FIG 2 Characterization of JEV(M-I36F) viral stocks. Wild-type JEV (WT) and mutant JEV(M-I36F) (I36F) viral stocks were amplified in C6/36 cells transfected with the respective infectious cDNA clones. (A) Viral stocks were collected from the C6/36 supernatants and titrated by FFA in BHK-21 or C6/36 cells. No foci were detected for the mutant virus when the FFA was performed in BHK-21 cells (n.d). The error bars represent the standard deviations of results from three independent transfections (for each transfection, the assays were done in duplicate). No statistically significant differences were found ($P > 0.05$). (B) The supernatants of infected C6/36 cells were analyzed for the presence of JEV E, C, and M proteins by Western blotting. A representative experiment out of >2 repeats is shown. (C) The specific infectivity of the virus released to the supernatant was calculated as the ratio of JEV RNA copies to FFU (obtained in C6/36 cells). The levels of JEV RNA copies present in the supernatants were quantified by RT-qPCR. Each of the experiments is represented by a different symbol, and the error bars represent the standard deviations of results of three independent experiments (for each experiment, the assays were done in duplicate). No statistically significant differences were found ($P > 0.05$).

and cloned into the similarly treated pTRE3G vector (Clontech; catalog no. 631173). The resulting pTRE3G-JEV-RP-9.prME plasmid was amplified in Stbl2 cells (Life Technologies; catalog no. 10268-019).

The M-I36F mutation was introduced directly in pTRE3G-JEV-RP-9.prME through PCR mutagenesis using primers 5′-CATGAAAACTGAGAACTGGTTCATAAGGAATCCTGGCTA-3′ and 5′-TAGCCAGGATTCCTTATGAACCAGTTCTCAGTTTTCATG-3′ (the mutation is underlined).

To produce JEV VLPs, HEK293T cells were transfected with pTRE3G-JEV-RP-9.prME or pTRE3G-JEV-RP-9.prME(M-I36F) using Lipofectamine 2000 (Life Technologies; catalog no. 11668-019) according to the manufacturer's instructions. The expression of the JEV structural genes was induced using the Tet-Express system (Clontech; catalog no. 631177) according to the manufacturer's instructions. The supernatants containing VLPs were collected at 24 h postinduction and clarified by centrifugation for 5 min at 1,000 × *g*. For VLP purification, the clarified supernatant was loaded over a sucrose cushion (15% sucrose in TNE [10 mM Tris-HCl, pH 7.5, 2.5 mM EDTA, 50 mM NaCl]) and centrifuged at 100,000 × *g* for 2.5 h at 4°C. The supernatants were discarded, and the purified VLPs were suspended in TNE buffer.

Mouse experiments. Three-week-old female C57BL/6 mice were housed under pathogen-free conditions at the Institut Pasteur animal facility. The protocols and subsequent experiments were ethically approved by the Ethic Committee for Control of Experiments on Animals (CETEA) at the Institut Pasteur and declared to the French Ministère de l'Enseignement Supérieur et de la Recherche (no. 000762.1) in accordance with European regulations. Experiments were conducted in accordance with the guidelines of the Office Laboratory of Animal Care at the Institut Pasteur. Groups of mice were intraperitoneally inoculated with various doses of JEV diluted in 100 μl of DPBS supplemented with 0.2% endotoxin-free serum albumin.

For the enzyme-linked immunosorbent assay (ELISA) and seroneutralization assay, the mice were bled by puncture at the retro-orbital sinus level. The blood was collected using a Capiject capillary blood collection tube (Terumo; catalog no. 3T-MG), and the serum was separated after centrifugation for 10 min at 4,000 × *g*.

Seroneutralization assay. The serum samples were 2-fold serially diluted in DMEM supplemented with 2% FBS, with a starting dilution of 1:20. Each dilution was incubated for 1 h at 37°C with 100 FFU of JEV-RP-9. The remaining infectivity was assayed on BHK-21 cells by FFA, as described above. Sera obtained from DPBS-inoculated mice served as the negative controls. Neutralization curves were generated and analyzed using GraphPad Prism. Nonlinear regression fitting with sigmoidal dose response (variable slope) was used to determine the serum dilution that reduced the number of FFU by 50% ($FRNT_{50}$).

Statistical analysis. An unpaired *t* test was used to compare quantitative data, and a log-rank (Mantel-Cox) test was used to compare survival data. GraphPad Prism was used for all statistical analyses.

RESULTS

Production of a JEV mutant carrying an isoleucine-to-phenylalanine substitution at position 36 in the M protein. To examine the role of the residue located at position M-36 in JEV infection, we mutagenized pBR322(CMV)-JEV-RP-9, a plasmid construct that bears an infectious full-length JEV-RP-9 cDNA clone (47). Accordingly, the isoleucine residue at position 36 of JEV M protein was mutated to phenylalanine. To produce viral stocks, *Aedes albopictus*-derived C6/36 cells were transfected with either pBR322(CMV)-JEV-RP-9(M-I36F) or wild-type pBR322(CMV)-JEV-RP-9. At 7 to 8 days posttransfection, the cells transfected with either plasmid displayed typical cytopathic effect corresponding to JEV production. The culture supernatants were collected, and the presence of the M-I36F mutation was verified by extraction of viral RNA from the supernatants, followed by RT-PCR and sequencing. Next, we quantified the amount of infectious virus produced using a standard FFA on hamster kidney-derived BHK-21 cells, but we were not able to detect any foci for the JEV(M-I36F) mutant virus (Fig. 2A, BHK-21). Interestingly, once we performed the same assay using C6/36 cells instead of BHK-21 cells, we were able to detect infection foci for the mutant virus (Fig. 2A, C6/36). Those foci did not display any obvious difference in size relative to the wild-type virus. We further characterized the viral stocks produced in C6/36 cells and observed that there were comparable accumulations of C, M, and E structural proteins in the supernatants of both wild-type and mutant viruses (Fig. 2B). In addition, we measured the levels of viral RNA in the supernatants and observed for both viruses a strict correlation with their infectious titers in C6/36 cells (Fig. 2C), which demonstrated that both viral stocks were produced with com-

parable efficiencies in C6/36 cells and had similar specific infectivities (Fig. 2C).

The mutation I36F in JEV M protein impairs viral production in mammalian cells but not in insect cells. Our characterization of the JEV(M-I36F) viral stocks led us to the interesting observation that this mutant virus was capable of developing infectious foci in C6/36 cells but not in BHK-21 cells (Fig. 2A). Consequently, we next decided to compare the impact of the M-I36F mutation on the JEV infectious cycle in insect cells with that in mammalian cells. C6/36 cells and the human neuroblastoma-derived SK-N-SH cells were infected with JEV(M-I36F) along with wild-type JEV (Fig. 3).

First, infected C6/36 cells were examined by immunofluorescence analysis (IFA) for JEV E protein expression at 24, 48, and 72 h postinfection (Fig. 3A). At 24 h postinfection, prior to virus spread, similar numbers of C6/36 cells were infected with both wild-type and mutant viruses, thus confirming comparable levels of infection efficiency (Fig. 3A, 24 h). Virus spread was observed at 48 and 72 h postinfection as a greater number of cells became infected with both viruses (Fig. 3A, 48 h and 72 h). Additionally, no significant difference in viral protein accumulation in C6/36 cell lysates was observed at 24 h and 48 h postinfection (Fig. 3B). Quantification of the infectious virus present in the culture supernatants at 24 and 48 h postinfection confirmed that the JEV(M-I36F) mutant could infect C6/36 cells with the same efficiency as the wild-type virus (Fig. 3C). Viral RNA was additionally extracted from the supernatants to evaluate the specific infectivity of the released virus, which was found to be similar for the two viruses (Fig. 3D and E).

We then performed a similar analysis of wild-type and mutant JEV infection in SK-N-SH cells (Fig. 3F to J). The IFA revealed that although at 24 h postinfection similar numbers of SK-N-SH cells were infected with each virus (Fig. 3F, 24 h), JEV(M-I36F) spread appeared less efficient at 48 and 72 h postinfection relative to that of the wild-type (Fig. 3F, 48 h and 72 h). Interestingly, in the SK-N-SH cells, while no significant difference in viral protein accumulation in cell lysates was observed over the time of infection (Fig. 3G), the level of infectious particles released to the supernatants was significantly lower for the mutant virus than for the wild-type (Fig. 3H). The analysis of RNA levels in the supernatants showed that there was conversely less viral RNA released from cells infected with the mutant virus than from those infected with the wild type (Fig. 3I). This observation indicated that lower levels of infectious viral particles were released after infection of SK-N-SH cells with JEV(M-I36F). Nonetheless, once we calculated the specific infectivity of each virus, we noted that the specific infectivity of JEV(M-I36F) was overall higher than that of the wild-type virus (Fig. 3J), thus implying that a certain level of noninfectious viral particles was released from SK-N-SH cells infected with JEV(M-I36F).

We also noted that the mutant virus JEV(M-I36F) was consistently affected in its infectious cycle when inoculated into various mammalian cell lines, such as BHK-21 or human kidney-derived HEK293T cells (data not shown). In contrast, we observed that the M-I36F mutation did not impact JEV infection of other insect cell lines, such as *Drosophila melanogaster*-derived S2 cells (data not shown). Overall these data demonstrated that the mutation M-I36F strongly impairs the JEV infectious cycle in mammalian cells but not in insect cells.

The mutation I36F in JEV M protein does not perturb the early stages of the viral cycle but affects the production of infectious virus. Since we observed that the mutant virus seemed to synthesize viral proteins at wild-type levels after inoculation into mammalian cells (Fig. 3F and G), we favored the hypothesis that this mutation did not affect the first steps of viral infection, such as entry, translation, and genome replication. To confirm this, we quantified the delivery of viral RNA into SK-N-SH cells at 1, 9, and 24 h after virus infection by calculating the relative accumulation of viral RNA to that of a host housekeeping mRNA (actin) (Fig. 4A). We observed that the mutant virus RNA accumulated in cells to levels comparable to that of the wild type, thus showing that genome delivery and replication were not readily affected by the mutation M-I36F (Fig. 4A).

Next, wild-type and mutant infectious cDNA clones were transfected into HEK293T cells, thus allowing us to bypass the viral entry into cells and evaluate the effects of the mutation on later stages of JEV infection. We analyzed the steady-state accumulation of viral proteins and noticed that although increasing amounts of protein were detected for both viruses, there was no significant difference in accumulation of structural proteins (prM and E) among viruses (Fig. 4B). The culture supernatants were collected at 24, 48, and 72 h posttransfection, and we observed that the levels of infectious virus were consistently low in the supernatants of the cells transfected with pBR322(CMV)-JEV-RP-9(M-I36F) (Fig. 4C). To determine if there was a defect in viral particle secretion from the transfected cells, we analyzed the culture supernatants by Western blotting. As shown in Fig. 4D and E, protein from JEV(M-I36F) was below detection levels in the supernatants. The levels of viral RNA detected in the supernatants were likewise found to be lower at all time points for the mutant virus (Fig. 4E), thus ultimately showing that low levels of viral particles were released from cells transfected with the pBR322(CMV)-JEV-RP-9(M-I36F) plasmid. Overall these data indicate that this mutation drastically prevents the release of infectious virus, even though viral RNA and proteins are clearly expressed within cells. Nonetheless, similarly to what we observed upon infection of SK-N-SH cells (Fig. 3J), we noted that the specific infectivity of the mutant virus released to the supernatants of transfected cells was significantly altered compared to that of the wild-type (Fig. 4F). This observation indicates that infection of mammalian cells with the mutant virus led to the release of noninfectious viral particles, which could partly contribute to the mutant virus phenotype.

The M-I36F mutation impairs the assembly and/or secretion of viral particles. To specifically address whether the M-I36F mutation affects JEV assembly and/or egress, we chose to examine its effect in a virus-like particle (VLP) system. Virus-like particles are particles that are naturally secreted during the virus infectious cycle (53) and are composed solely of prM and E proteins embedded in a lipid membrane. This system allows us to study defects in viral assembly and secretion, since these VLPs are produced independently of viral RNA replication (54). The M-I36F mutation was introduced into the VLP expression plasmid pTRE3G-JEV-RP-9.prME, which directs the expression of JEV-RP-9 prM and E proteins upon induction with the Tet-Express reagent. HEK293T cells were transfected with the resulting plasmid, using the wild-type plasmid as a control, and the viral protein expression was induced the next day. At 24 h postinduction, the intracellular expression of E and prM proteins and the release of VLPs to the supernatants

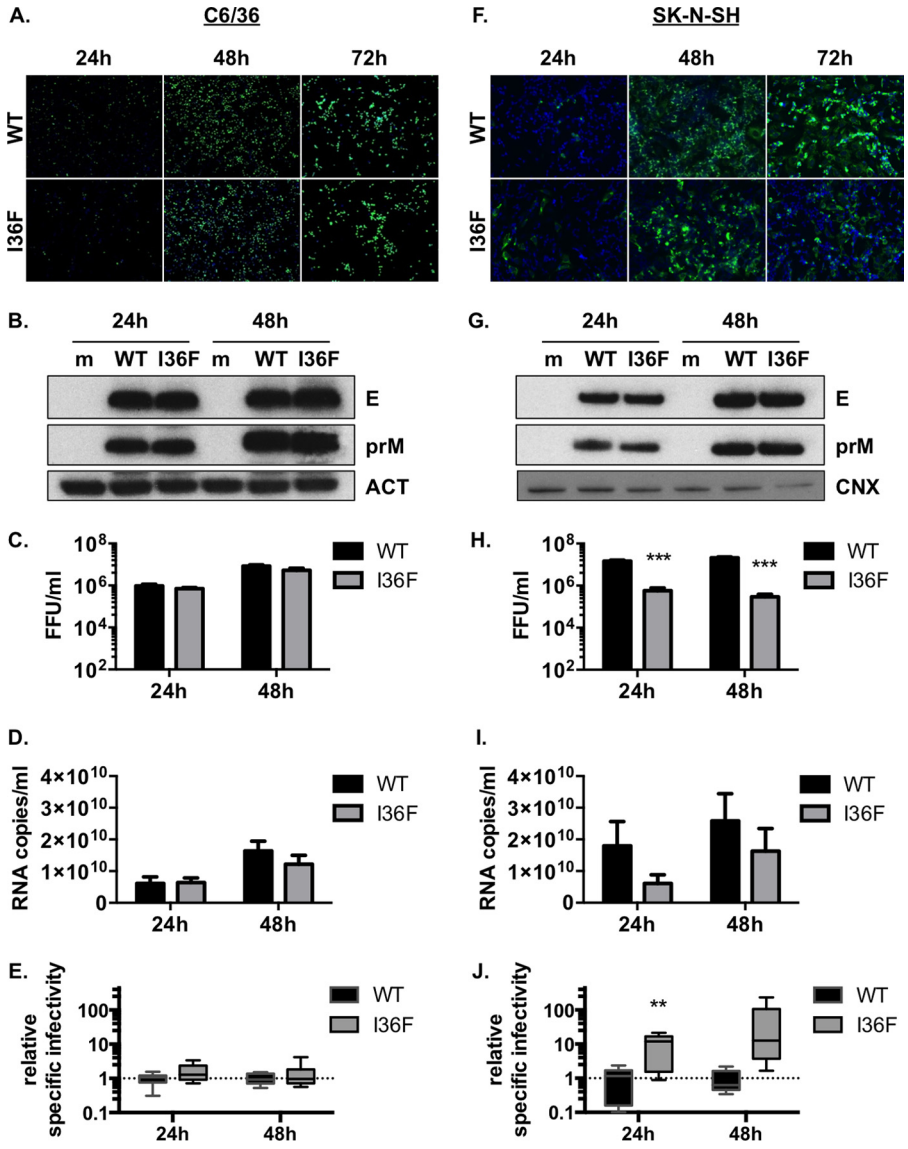

FIG 3 The JEV(M-I36F) infectious cycle is impaired in mammalian cells but not in insect cells. Mosquito-derived C6/36 cells (A, B, C, D, E) or human neuroblastoma-derived SK-N-SH cells (F, G, H, I, J) were infected with wild-type JEV (WT) or mutant JEV(M-I36F) (I36F) at a multiplicity of infection (MOI) of 1 (A, F) or at an MOI of 5 (B, C, D, E, G, H, I, J). Representative experiments out of >2 repeats are shown. (A and F) The infected cells were analyzed at 24, 48, or 72 h postinfection by immunofluorescence staining for the presence of the E protein (green). The images were taken at a ×100 (A) or ×200 (F) magnification. (B and G) The cell lysates of C6/36 (B) or SK-N-SH (G) cells were analyzed at 24 and 48 h postinfection for the presence of JEV E and prM proteins, as well as actin (ACT) or calnexin (CNX), by Western blotting. Mock-infected cells (m) served as a control. (C and H) The infectious virus released to the supernatants at 24 and 48 h postinfection was quantified by FFA in C6/36 cells. The error bars represent the standard deviations of results of three independent experiments (for each experiment, the assays were done in triplicate). Asterisks indicate that the differences between wild-type and mutant samples are statistically significant when the data are compared at each time point using the unpaired *t* test (***, $P < 0.001$; **, $0.001 < P < 0.01$; *, $0.01 < P < 0.05$; only statistically significant differences are shown). (D and I) Viral RNA was extracted from the cell supernatants, and JEV RNA copies were quantified by RT-qPCR. The error bars represent the standard deviations of results of three independent experiments (for each experiment, the assays were done in triplicate). Asterisks indicate that the differences between experimental samples are statistically significant when the data are compared at each time point using the unpaired *t* test (***, $P < 0.001$; **, $0.001 < P < 0.01$; *, $0.01 < P < 0.05$; only statistically significant differences are shown). (E and J) The relative specific infectivity of the virus released to the supernatant was measured as a function of the specific infectivity obtained for the wild-type virus in each experiment. The specific infectivity was calculated as the ratio of JEV RNA copies to FFU. The error bars represent the standard deviations of results of three independent experiments (for each experiment, the assays were done in triplicate). Asterisks indicate that the differences between experimental samples are statistically significant when the data are compared at each time point using the unpaired *t* test (***, $P < 0.001$; **, $0.001 < P < 0.01$; *, $0.01 < P < 0.05$; only statistically significant differences are shown).

were monitored by Western blotting (Fig. 5A). Interestingly, the presence of the mutation M-I36F led to a strong decrease in VLP secretion (Fig. 5A, lower panel). This decrease did not result from a reduced steady-state expression of prM and/or E, since no obvious difference in intracellular abundance of these proteins was observed between wild-type and mutant transfections (Fig. 5A, top panel). This result was consistent with data obtained with transfection of the full-length infectious clone

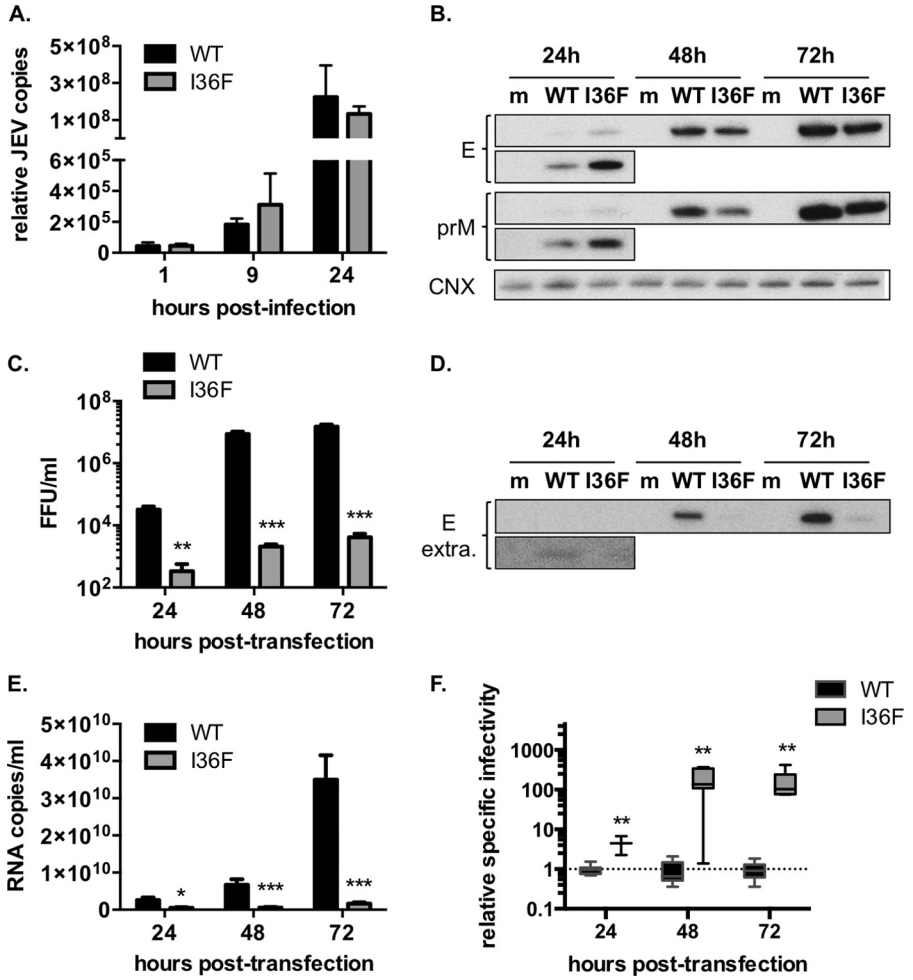

FIG 4 The M-I36F mutation has no effect on JEV entry and RNA replication, but it perturbs the late stages of viral production. (A) SK-N-SH cells were infected with wild-type JEV (WT) or mutant JEV(M-I36F) (I36F) at an MOI of 1. A representative experiment out of 2 repeats is shown. JEV RNA copies accumulating in infected cells were quantified by RT-qPCR. The results were normalized to actin mRNA and are expressed as the relative fold increase over RNA from mock-infected controls. The error bars represent the standard deviations of results of the experiment (the assays were done on duplicate experimental samples). (B, C, D, E) Human kidney-derived HEK293T cells were transfected with the wild-type pBR322(CMV)-JEV-RP-9 cDNA clone (WT) or with the mutant pBR322(CMV)-JEV-RP-9(M-I36F) cDNA clone (I36F). (B) The cell lysates were analyzed at 24, 48, and 72 h posttransfection for the presence of JEV E and prM proteins, as well as calnexin (CNX), by Western blotting. Mock-transfected cells (m) served as a control. The lower inset corresponds to a higher exposure of the blot. A representative experiment out of >2 repeats is shown. (C) The infectious virus released to the supernatants at 24, 48, and 72 h posttransfection was quantified by FFA in C6/36 cells. The error bars represent the standard deviations of results of three independent experiments (for each experiment, the assays were done in triplicate). Asterisks indicate that the differences between experimental samples are statistically significant when data are compared at each time point using the unpaired *t* test (***, $P < 0.001$; **, $0.001 < P < 0.01$; *, $0.01 < P < 0.05$; not significant, $P > 0.05$). (D) The cell supernatants were analyzed at 24, 48, and 72 h posttransfection for the presence of JEV E protein by Western blotting. Mock-transfected cells (m) served as a control. The lower inset corresponds to a higher exposure of the blot. A representative experiment out of >2 repeats is shown. (E) Viral RNA was extracted from the cell supernatants, and JEV RNA copies were quantified by RT-qPCR. The error bars represent the standard deviations of results of three independent experiments (for each experiment, the assays were done in triplicate). Asterisks indicate that the differences between experimental samples are statistically significant when data are compared at each time point using the unpaired *t* test (***, $P < 0.001$; **, $0.001 < P < 0.01$; *, $0.01 < P < 0.05$; not significant, $P > 0.05$). (F) The relative specific infectivity of the virus released to the supernatant was measured as a function of the specific infectivity obtained for the wild-type virus in each experiment. The specific infectivity was calculated as the ratio of JEV RNA copies to FFU. The error bars represent the standard deviations of results of three independent experiments (for each experiment, the assays were done in triplicate). Asterisks indicate that the differences between experimental samples are statistically significant when data are compared at each time point using the unpaired *t* test (***, $P < 0.001$; **, $0.001 < P < 0.01$; *, $0.01 < P < 0.05$; not significant, $P > 0.05$).

(Fig. 4B to E) and confirmed that the mutation M-I36F impairs assembly and/or secretion of VLPs in mammalian cells.

Such defects in flavivirus assembly are often caused by an improper interaction of prM/M with E, which either affects the heterodimer formation or interferes with the structural changes needed during the process of flavivirus particle maturation (31, 33–35, 55, 56). To test whether the M-I36F mutation impairs the interaction between prM and E in mammalian cells, we examined the association of E and prM proteins in lysates obtained from BHK-21 cells infected with the wild-type or mutant virus. We used an anti-E monoclonal antibody to pull down JEV E proteins and then probed the immunoprecipitates for the presence of E and prM proteins (Fig. 5B). As expected, prM was detected in the wild-type E pulldown (Fig. 5B). When we analyzed the cells infected with JEV(M-I36F), the ratio of prM to the E protein was similar to that observed for the wild-type infection (Fig. 5B). This

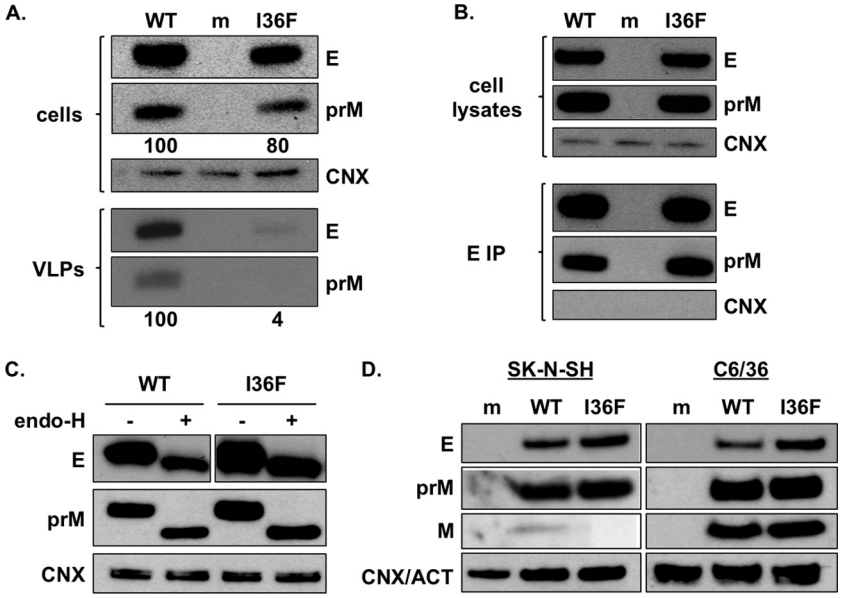

FIG 5 In mammalian cells, the M-I36F mutation impairs viral particle assembly and/or secretion. (A) HEK293T cells were transfected with pTRE3G-JEV-RP-9.prME (WT) or pTRE3G-JEV-RP-9.prME(M-I36F) (I36F) plasmids. The cells and supernatant contents were analyzed 24 h after induction of gene expression. A representative experiment out of >3 repeats is shown. In the top panel (cells), the cell lysates were analyzed for the presence of JEV E and prM proteins, as well as calnexin (CNX), by Western blotting. Mock-transfected cells (m) served as a control. In the lower panel (VLPs), the VLPs released in the supernatants were purified and analyzed by Western blotting for the presence of JEV E and prM proteins. Supernatants collected from mock-transfected cells (m) served as a control. The combined levels of prM and E accumulating in cell lysates and in purified VLPs were quantified using ImageJ and normalized to the wild type. The quantification results are indicated below each panel. (B) BHK-21 cells were infected with wild-type JEV (WT) or mutant JEV(M-I36F) (I36F) at an MOI of 5. A representative experiment out of 2 repeats is shown. The steady-state expression of prM and E proteins was monitored in the cell lysates at 24 h postinfection, using calnexin (CNX) as a loading control (top). The cell lysates were immunoprecipitated (IP) using an antibody specific for JEV E protein. The immunoprecipitates (bottom) were analyzed by Western blotting to confirm that the JEV E protein had been captured by immunoprecipitation. The JEV prM protein was also detected in the immunoprecipitates, whereas CNX was undetectable, showing that the prM coimmunoprecipitation was specific. (C) SK-N-SH cells were infected with wild-type JEV (WT) or mutant JEV(M-I36F) (I36F) at an MOI of 5. A representative experiment out of 2 repeats is shown. Cell lysates were collected at 24 h postinfection and treated with endo-H and then analyzed by Western blotting for the presence of JEV E and prM proteins, as well as calnexin (CNX). (D) SK-N-SH and C6/36 cells were infected with wild-type JEV (WT) or mutant JEV(M-I36F) (I36F) at an MOI of 5. Cell lysates were collected at 48 h postinfection and analyzed by Western blotting for the presence of E, prM, and M proteins, as well as calnexin (CNX) or actin (ACT) as a loading control for SK-N-SH or C6/36 cell lysates, respectively.

provides biochemical evidence that the prM/E heterodimerization was not affected by the M-I36F mutation and was not responsible for the lack of viral particle assembly within mammalian cells.

To test whether the mutant prM protein was posttranslationally modified and was able to traffic through the secretory pathway, we collected SK-N-SH cell lysates at 24 h after viral infection and treated them with endo-H, an enzyme that removes immature high-mannose glycans from proteins. These sugars are added to proteins in the ER and are trimmed and further modified in the Golgi apparatus, conferring resistance to endo-H (57). As shown in Fig. 5C, we could not detect any pool of glycoproteins associated with the Golgi apparatus within mammalian cells infected with either virus. While this experiment did not allow us to elucidate whether prM intracellular trafficking was affected by the M-I36F mutation, it showed that the mutant prM protein glycosylation pattern was not affected in mammalian cells, relative to that of the wild type.

Next, we analyzed the impact of the mutation on later stages of viral assembly, such as the processing of prM protein during virion maturation. C6/36 cells and SK-N-SH cells were infected with JEV(M-I36F) along with wild-type JEV, and we examined the accumulation of prM and M proteins in cells at 48 h postinfection (Fig. 5D). Since prM is cleaved into pr and M by furin in the *trans*-Golgi apparatus (12, 17–19), this assay allowed us to simultaneously evaluate the effect of the M-I36F mutation on virus intracellular trafficking and on the maturation process. As observed before, the mutant prM proteins accumulated to levels that were similar to or higher than those of the wild type in mammalian cells (Fig. 5D). Interestingly, while we could detect low levels of M proteins in SK-N-SH cells infected with the wild-type virus, the accumulation of the mutant M protein was below detection levels (Fig. 5D, left panel). In C6/36 cells, the JEV M protein was found to accumulate to high levels, and we did not observe any difference in prM or M accumulation between the wild-type and mutant viruses (Fig. 5D, right panel). This observation indicates that the mutant prM protein was not readily accessible to furin cleavage in mammalian cells.

JEV(M-I36F) is attenuated *in vivo* and induces production of JEV neutralizing antibodies in mice. To investigate whether the defect in JEV(M-I36F) infection of mammalian cells *in vitro* could result in viral attenuation *in vivo*, we evaluated the ability of the virus to induce viral pathogenesis in a murine model for Japanese encephalitis (47). Three-week-old female C57BL/6 mice were injected intraperitoneally with a single dose of 10^3 FFU of the parental virus or with 10^3 to 10^6 FFU of the JEV(M-I36F) virus (Fig. 6A). C57BL/6 mice are highly susceptible to JEV infection, and accordingly, after injection with the wild-type virus, the animals rapidly

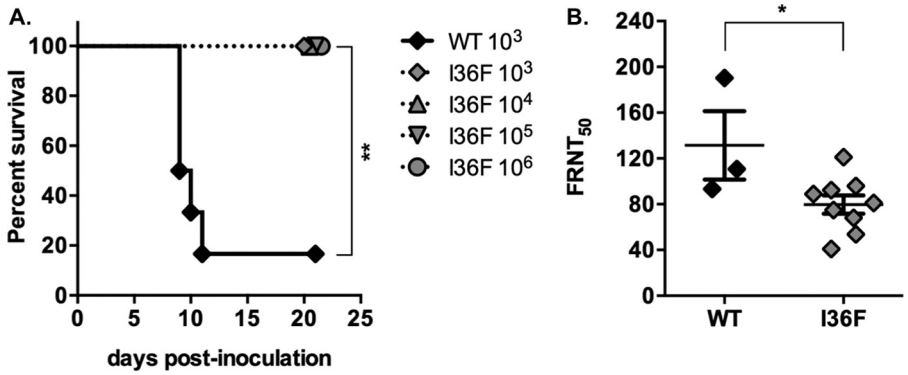

FIG 6 JEV(M-I36F) is attenuated *in vivo* and induces the production of JEV neutralizing antibodies in mice. (A) Groups of 3-week-old C57BL/6 mice (6 per group) were monitored for survival after intraperitoneal injection with various doses (10^3 to 10^6 FFU) of wild-type JEV (WT) or mutant JEV(M-I36F) (I36F). A representative experiment out of 2 repeats is shown. Asterisks indicate that the differences between survival curves are statistically significant when data are compared using the log-rank (Mantel-Cox) test (***, $P < 0.001$; **, $0.001 < P < 0.01$; *, $0.01 < P < 0.05$; not significant, $P > 0.05$). (B) The neutralization activities against wild-type live JEV of sera collected from C57BL/6 mice 23 days after inoculation with 10^3 FFU of wild-type JEV (WT) or mutant JEV(M-I36F) (I36F) were evaluated using a standard FRNT assay in BHK-21 cells. Each symbol represents the $FRNT_{50}$ value obtained for an individual mouse. Asterisks indicate that the differences between experimental samples are statistically significant when data are compared using the unpaired *t* test (***, $P < 0.001$; **, $0.001 < P < 0.01$; *, $0.01 < P < 0.05$; not significant, $P > 0.05$).

developed symptoms typically associated with central nervous system invasion, such as limb paralysis and encephalitis. The survival rate was between 0 and 16.7%, with a mean survival time of 11.5 days (Fig. 6A). In contrast, the mice injected with increasing doses of the mutant virus did not develop any symptoms and survived the infection, even when the inoculation dose was as high as 10^6 FFU (Fig. 6A). These data indicate that JEV(M-I36F) is greatly attenuated in C57BL/6 mice.

The sera were collected from all surviving mice at 27 days postinoculation, and the JEV-specific antibody endpoint titers were quantified by ELISA. We found that all of the mice surviving JEV(M-I36F) infection had produced high levels of IgG antibodies against JEV (data not shown). Next, we evaluated the neutralization potency of those antibodies in a seroneutralization assay. We observed that the sera collected from JEV(M-I36F)-inoculated mice had potent neutralizing activity against JEV, although the titers of neutralizing antibodies were slightly higher in sera obtained from mice inoculated with the wild-type virus (Fig. 6B). Taken together, these data show that the introduction of a single mutation that affects the late stages of JEV infection, such as assembly/secretion of viral particles, completely abrogates viral pathogenesis in a mouse model without interfering with the induction of the humoral immune response to JEV.

DISCUSSION

The M-I36F mutation affects JEV assembly and/or secretion in mammalian cells. In this study, we have demonstrated that the introduction of a single mutation in the M protein of JEV leads to a severe reduction in infectious particle production from mammalian cells. Our experiments suggested that the M-I36F mutation did not directly affect entry, since we showed that upon infection with viral particles produced in insect cells, the RNA delivery and the steady-state protein production were unaffected during the first cycle of mammalian cell infection (Fig. 4A and 3F and G, 24 h). Additionally, we noted that while the production of infectious virus from mammalian cells appeared to be affected, some of the progeny virus seemed to have conserved the capacity to infect naive cells, as there was a limited but detectable spread of viral antigens from 24 to 72 h postinfection (Fig. 3F). Importantly, we noted that while some of the mutant viral progeny produced from mammalian cells was fully competent at infecting naive C6/36 cells, a significant proportion of viral particles released to the supernatants of mammalian cells was noninfectious (Fig. 3J and 4F). However, given that this was not the case for viral particles released from insect cells (Fig. 3E), it is likely that this reflects an impact of the mutation on the formation of infectious viral particles from mammalian cells rather than on the entry process.

Along these lines, we showed that the JEV(M-I36F) defect was linked to a strong decrease in the secretion of viral particles from mammalian cells, either genuine virions (Fig. 4D) or VLPs composed solely of prM/M and E (Fig. 5A). Specific residues in the M protein, in particular ones that are located in the helix domain (residues 21 to 40 [Fig. 1B]), have already been shown to be critical for proper flavivirus assembly (16, 30–35, 55, 56). Of note, a residue close to M-I36, residue M-E33, is part of an interaction network with domain II of the E protein, and mutagenesis of this residue affects the formation of JEV viral particles in insect and mammalian cells (33). We were able to show that the M-I36F mutation did not affect some of the processes known to be important for viral assembly in mammalian cells, such as heterodimer formation (Fig. 5B) (31, 33–35, 55, 56) or prM glycosylation (Fig. 5C) (50), but seemed to interfere with the processing of prM protein into pr and M (Fig. 5D).

Flavivirus particle production relies on prM cleavage by furin in the *trans*-Golgi apparatus, and this maturation process is a prerequisite to the production of infectious flavivirus particles (21, 22). The fact that the processing of prM into M in mammalian cells was affected for the mutant virus (Fig. 5D) argues for a defect in viral particle maturation and is in agreement with the observation that noninfectious viral particles were released from mammalian cells infected with JEV(M-I36F) (Fig. 3J and 4F). However, while optimal cleavage of prM has been previously shown to be important for assembly of infectious viral particles, it generally has not been shown to impact their secretion (16, 31, 55, 58). Consequently, it seems unlikely that a sole defect in maturation is responsible for the drastic loss of mutant viral particles released to

mammalian cell supernatants (Fig. 4D and 5A). We therefore favor the hypothesis that the lack of mutant M protein accumulation within mammalian cells (Fig. 5D) is due to a block of prM trafficking to the *trans*-Golgi apparatus that prevents its processing through furin into pr and M. The higher production of immature viral particles would then be an additional consequence of this defect.

The M-I36F mutation causes a host-dependent phenotype. One central finding of our work is that the JEV(M-I36F) mutant virus has a host-dependent phenotype. The M-I36F mutation strongly impaired viral production in mammalian cells, while it had no detectable effect on the infection of insect cells (Fig. 3). An explanation for the differential phenotype of the M-I36F mutation may come from the physical properties of virions grown in each cell type. It is known that for some strains of DV, the virions adopt different structures when grown at 28°C (as in insect cells) or above 33°C (as in mammalian cells) (59–61). While studies on the impact of temperature on JEV structure are currently lacking, it is likely that the introduction of a mutation would exert different constraints if the viral particle adopts temperature-dependent structures. We evaluated the impact of temperature by testing viral particle secretion from mammalian cells grown at 30°C and still observed a reduction in mutant VLP secretion relative to that of the wild type (data not shown). Other experiments involving the infection of wild-type or mutant JEV in either mammalian cells grown at 30°C or mosquito cells grown at 37°C were difficult to interpret due to high cellular cytotoxicity and reduced viral growth (data not shown). The development of alternative assays is therefore needed to definitively assess the effect of temperature on the mutant phenotype.

In flaviviruses, specific mutations in viral RNA and proteins have been involved in host dependence at various stages of the infectious cycle (62–66). In a specific instance, the inhibition of E glycosylation in tick-borne encephalitis virus (TBEV) had no impact on virion secretion from tick cells, while it strongly impaired secretion from mammalian cells (66), an observation that may be linked to the finding that TBEV appears to follow a noncanonical secretion pathway in tick cells (67). In the case of mosquito-borne flaviviruses, virions are generally thought to be secreted through the Golgi apparatus, in both mosquito and mammalian cells (68), although some alternate budding at the plasma membrane of C6/36 cells was observed for West Nile virus (WNV) (69) and DV (70). While the existence of such noncanonical secretion needs to be further addressed, it is evident that flavivirus infection induces different ultrastructural changes in mammalian cells than in mosquito cells (9, 68). Thus, in the case of JEV, the difference in phenotype observed for the JEV(M-I36F) mutant could account for differences in viral trafficking pathways existing among hosts.

Additionally, it is possible that the mutation M-I36F impairs a direct interaction with a mammalian cellular factor involved in virion assembly or secretion. While there are limited data on insect host proteins interacting with flavivirus prM/M (38), several interacting proteins were identified in mammalian cells, such as members of the ADP-ribosylation factor (39), vacuolar ATPases (40), a light chain of dynein (36), a DEAD box helicase, FUNDC1/2 (37), and claudin-1 (41). In some cases, this interaction was even involved in viral particle secretion (39, 40). Even though those mammalian prM/M interacting proteins have orthologs in insects, the strength of such an interaction could differ among hosts and be more or less sensitive to the introduction of mutations in the M protein. Further study of this type of mutations could therefore help dissect the contribution of host components in the JEV infectious cycle.

Importance of the nature of the M-36 residue in flaviviruses. Interestingly, we observed that the nature of the amino acid at position 36 was crucial for proper viral particle production, since the introduction of an alanine mutation at position M-36 in JEV did not impact the virus infectious cycle in mammalian and insect cells or VLP production from mammalian cells (data not shown). It was also shown by others that such M-I36A mutation did not affect JEV VLP production from Sf9 insect cells (33). On the other hand, the substitution of alanine for isoleucine at position M-36 in DV4 resulted in a slight decrease in VLP production from mammalian cells (32). In DV, other substitutions at position M-36 that replaced an isoleucine (DV2 and DV4) or an alanine (DV1) with a proline led to a drastic decrease in VLP production from mammalian cells (32). When introduced in a DV2 infectious clone, this residue was rapidly replaced by a leucine (32). In flaviviruses, position 36 is occupied either by an isoleucine (JEV, WNV, DV2, and DV4), an alanine (DV1 and DV3), or a leucine (wild-type YFV), all of those being aliphatic hydrophobic residues (Fig. 1B). While proline is known to have an exceptional conformational rigidity that is likely to disturb the M helix structure, phenylalanine properties are closer to those of the amino acids originally found at position M-36. Importantly, phenylalanine is also hydrophobic and therefore is likely to be buried in the protein structure in the same manner as the original residues. However, phenylalanine is an aromatic residue and therefore could interact with nonprotein ligands, as its aromatic side chain could be involved in stacking interactions with other aromatic side chains (71). The intrinsic properties of this amino acid might therefore contribute in yet undefined ways to the M-I36F mutant phenotype.

Interestingly, wild-type strains of YFV all have a leucine at position M-36, whereas both vaccine strains YFV-17D and YFV-FNV have a phenylalanine at this position (72) (Fig. 1B). While both vaccine strains were attenuated relative to the wild-type YFV, they were fully competent at forming viral particles, which raises the question as to why a similar mutation would affect JEV assembly but not that of YFV. Accordingly, the introduction of this sole mutation in a wild-type YFV strain did not seem to have any effect on viral production in mammalian cells (45). It is thus possible that residues specifically found in YFV—and absent in JEV—render that virus insensitive to the presence of the M-L36F mutation. Alternatively, we note that the two YFV vaccine strains carry additional mutations in several other proteins that could compensate for a defect in particle assembly (44, 72). Notably, several amino acid changes have accumulated in domain II of the E protein (G52R, A54V, A56V, Y61S, K200T, N249D), a region shown to interact with the M helix domain in JEV (33). While growing virus, we noted that the mutation was reverted after two passages on mammalian cells, but we did not observe the presence of any compensatory mutations in the structural proteins (nucleotides 83 to 2235) that would restore viral particle assembly (data not shown). It could be interesting to analyze further the virus population arising after several passages in those cells: this could shed a light on how interactions with other viral proteins are important in the process of assembly.

Rational design of a live-attenuated vaccine. One important finding of our study was that the JEV M-I36F mutant was attenuated *in vivo* and that mice injected with mutant virus produced

JEV neutralizing antibodies (Fig. 6). Interestingly, the homologous mutation M-L36F is one of the 32 amino acid substitutions differentiating the wild-type Asibi strain from the 17D vaccine strain (44). Historically, the first live attenuated flavivirus vaccine (YFV-17D) was developed against YFV and confers remarkable and durable protection after a single-dose immunization (73). This vaccine strain has also been used for the development of live attenuated chimeric viruses designed to confer immunity against other flaviviruses, such as DV, WNV, or JEV (74, 75). Surprisingly, the specific molecular basis of YFV-17D attenuation is not yet fully understood. Reasonably, it was hypothesized that the set of mutations differentiating the Asibi and 17D strains represent determinants of mammalian pathogenicity (76). However, recent work by Beck and coworkers demonstrated that a loss of population diversity may be a factor in YFV-17D attenuation, since wild-type virus consists of highly diverse quasispecies, whereas the vaccine strain population is homogeneous (77).

The success of the YFV-17D vaccine has led to multiple attempts at producing live attenuated vaccines against other flaviviruses (78). In the case of JEV, a live attenuated JEV vaccine, SA_{14}-14-2, was developed in China and has been successfully used for decades in China and now in other Asian countries (79, 80), although it is not recommended for global use due to a theoretical risk for reversion to neurovirulence. There again, the molecular basis of JEV-SA_{14}-14-2 attenuation is unclear. Two mutations in the E protein were found as important factors: the mutation E138K was involved in viral clearance (81) and interferon antagonism (46), while the mutation E244G was recently linked to neurovirulence attenuation (82). Additionally JEV-SA_{14}-14-2 did not appear to produce the NS1′ protein (83), an important factor in viral neuroinvasiveness (84).

Thus, while YFV-17D and JEV-SA_{14}-14-2 are both successful vaccines, the molecular bases for their attenuation remain unclear and may be caused by multiple, cumulative changes. While many live attenuated vaccines were created empirically, new approaches for developing such vaccines could be based on rational design of attenuating mutations that affect the virus infectious cycle or its interaction with the host (85). Our results demonstrate that it is possible to induce attenuation by a single mutation that impacts assembly and/or egress of a pathogenic JEV strain in mammalian cells. We noted that this mutant virus elicited the production of neutralizing anti-JEV antibodies in challenged mice (Fig. 6B), thus suggesting that its immunogenicity was not abrogated. Accordingly, we had noted that this mutant was not entirely deficient at producing progeny virus *in vitro* (Fig. 3G). It is thus likely that this was also the case *in vivo* and that the mutant virus was recognized by the host immune system prior to its clearance from the bloodstream. Since early viremia in blood is known to be important for successful invasion of the central nervous system by JEV and by related flaviviruses (86–89), the virus would have to mutate at this early stage of infection in order to develop pathogenesis. Importantly, we found that no viral RNA could be detected in the blood or in the organs (brain, liver, spleen, kidney) of mice inoculated with the mutant virus, thus suggesting that the virus was most likely cleared before reversion to a wild-type phenotype could occur *in vivo* (data not shown). The latter observation also demonstrated that the induction of the immune response was not linked to a low level of viral propagation in the animal.

The M-I36F mutation thus provides a good path to make a successful vaccine: it does not present timely reversion, it affects the infectious cycle at a known stage, and it elicits a good immune response in animals. It could be interesting to introduce this mutation in a JEV vaccine strain, such as SA_{14}-14-2, and observe whether the introduction of this mutation reduces the frequency of adverse events while keeping the vaccine's efficiency. Since a homologous mutation identified in YFV vaccine strains has never been associated with their attenuation phenotype, this study poses the question as to what is the exact role of this mutation in YFV attenuation. Additionally, our work has highlighted the host-dependent importance of a residue in the M protein in viral assembly and/or secretion and thus opens new avenues to study the role of this small protein in the infectious cycle of flaviviruses.

ACKNOWLEDGMENTS

We thank Priscilla L. Yang for support, Yi-Lin Ling for providing the JEV-RP-9 cDNA clone, Yoshiharu Matsuura for providing the anti-JEV C antibody, and Young-Min Lee for providing the anti-JEV M antibody.

FUNDING INFORMATION

Seventh Framework Programme (FP7) provided funding to Melissanne de Wispelaere under grant number 278433-PREDEMICS. Ministry of Defence | Direction Générale de l'Armement (DGA) provided funding to Cécile Khou. HHS | NIH | National Institute of Allergy and Infectious Diseases (NIAID) provided funding to Melissanne de Wispelaere under grant number NIH/NIAID U19AI109740.

REFERENCES

1. **Lindenbach BD, Thiel H-J, Rice CM.** 2007. Flaviviridae: the viruses and their replication, p 1101–1152. *In* Knipe DM, Howley PM (ed), Fields virology. Lippincott Williams & Wilkins, Philadelphia, PA.
2. **Campbell GL, Hills SL, Fischer M, Jacobson JA, Hoke CH, Hombach JM, Marfin AA, Solomon T, Tsai TF, Tsu VD, Ginsburg AS.** 2011. Estimated global incidence of Japanese encephalitis: a systematic review. Bull World Health Organ **89:**766–774, 774A–774E. http://dx.doi.org/10.2471/BLT.10.085233.
3. **Fischer M, Hills S, Staples E, Johnson B, Yaich M, Solomon T.** 2008. Japanese encephalitis prevention and control: advances, challenges, and new initiatives, p 93–124. *In* Scheld WM, Hammer SM, Hughes JM (ed), Emerging infections 8. ASM Press, Washington, DC.
4. **Zhu Y-Z, Xu Q-Q, Wu D-G, Ren H, Zhao P, Lao W-G, Wang Y, Tao Q-Y, Qian X-J, Wei Y-H, Cao M-M, Qi Z-T.** 2012. Japanese encephalitis virus enters rat neuroblastoma cells via a pH-dependent, dynamin and caveolae-mediated endocytosis pathway. J Virol **86:**13407–13422. http://dx.doi.org/10.1128/JVI.00903-12.
5. **Kalia M, Khasa R, Sharma M, Nain M, Vrati S.** 2013. Japanese encephalitis virus infects neuronal cells through a clathrin-independent endocytic mechanism. J Virol **87:**148–162. http://dx.doi.org/10.1128/JVI.01399-12.
6. **Allison SL, Schalich J, Stiasny K, Mandl CW, Heinz FX.** 2001. Mutational evidence for an internal fusion peptide in flavivirus envelope protein E. J Virol **75:**4268–4275. http://dx.doi.org/10.1128/JVI.75.9.4268-4275.2001.
7. **Modis Y, Ogata S, Clements D, Harrison SC.** 2004. Structure of the dengue virus envelope protein after membrane fusion. Nature **427:**313–319. http://dx.doi.org/10.1038/nature02165.
8. **Gillespie LK, Hoenen A, Morgan G, Mackenzie JM.** 2010. The endoplasmic reticulum provides the membrane platform for biogenesis of the flavivirus replication complex. J Virol **84:**10438–10447. http://dx.doi.org/10.1128/JVI.00986-10.
9. **Junjhon J, Pennington JG, Edwards TJ, Perera R, Lanman J, Kuhn RJ.** 2014. Ultrastructural characterization and three-dimensional architecture of replication sites in dengue virus-infected mosquito cells. J Virol **88:**4687–4697. http://dx.doi.org/10.1128/JVI.00118-14.
10. **Welsch S, Miller S, Romero-Brey I, Merz A, Bleck CKE, Walther P, Fuller SD, Antony C, Krijnse-Locker J, Bartenschlager R.** 2009. Composition and three-dimensional architecture of the dengue virus replication and assembly sites. Cell Host Microbe **5:**365–375. http://dx.doi.org/10.1016/j.chom.2009.03.007.

11. **Konishi E, Mason PW.** 1993. Proper maturation of the Japanese encephalitis virus envelope glycoprotein requires cosynthesis with the premembrane protein. J Virol **67:**1672–1675.
12. **Yu I-M, Zhang W, Holdaway HA, Li L, Kostyuchenko VA, Chipman PR, Kuhn RJ, Rossmann MG, Chen J.** 2008. Structure of the immature dengue virus at low pH primes proteolytic maturation. Science **319:**1834–1837. http://dx.doi.org/10.1126/science.1153264.
13. **Kostyuchenko VA, Zhang Q, Tan JL, Ng T-S, Lok S-M.** 2013. Immature and mature dengue serotype 1 virus structures provide insight into the maturation process. J Virol **87:**7700–7707. http://dx.doi.org/10.1128/JVI.00197-13.
14. **Zhang Q, Hunke C, Yau Y-H, Seow V, Lee S, Tanner LB, Guan XL, Wenk MR, Fibriansah G, Chew PL, Kukkaro P, Biukovic G, Shi P-Y, Shochat SG, Grüber G, Lok S-M.** 2012. The stem region of premembrane protein plays an important role in the virus surface protein rearrangement during dengue maturation. J Biol Chem **287:**40525–40534. http://dx.doi.org/10.1074/jbc.M112.384446.
15. **Zhang X, Ge P, Yu X, Brannan JM, Bi G, Zhang Q, Schein S, Zhou ZH.** 2013. Cryo-EM structure of the mature dengue virus at 3.5-Å resolution. Nat Struct Mol Biol **20:**105–110. http://dx.doi.org/10.1038/nsmb.2463.
16. **Zheng A, Yuan F, Kleinfelter LM, Kielian M.** 2014. A toggle switch controls the low pH-triggered rearrangement and maturation of the dengue virus envelope proteins. Nat Commun **5:**3877. http://dx.doi.org/10.1038/ncomms4877.
17. **Li L, Lok S-M, Yu I-M, Zhang Y, Kuhn RJ, Chen J, Rossmann MG.** 2008. The flavivirus precursor membrane-envelope protein complex: structure and maturation. Science **319:**1830–1834. http://dx.doi.org/10.1126/science.1153263.
18. **Shapiro D, Brandt WE, Russell PK.** 1972. Change involving a viral membrane glycoprotein during morphogenesis of group B arboviruses. **50:**906–911.
19. **Stadler K, Allison SL, Schalich J, Heinz FX.** 1997. Proteolytic activation of tick-borne encephalitis virus by furin. J Virol **71:**8475–8481.
20. **Yu I-M, Holdaway HA, Chipman PR, Kuhn RJ, Rossmann MG, Chen J.** 2009. Association of the pr peptides with dengue virus at acidic pH blocks membrane fusion. J Virol **83:**12101–12107. http://dx.doi.org/10.1128/JVI.01637-09.
21. **Elshuber S, Allison SL, Heinz FX, Mandl CW.** 2003. Cleavage of protein prM is necessary for infection of BHK-21 cells by tick-borne encephalitis virus. J Gen Virol **84:**183–191. http://dx.doi.org/10.1099/vir.0.18723-0.
22. **Zybert IA, van der Ende-Metselaar H, Wilschut J, Smit JM.** 2008. Functional importance of dengue virus maturation: infectious properties of immature virions. J Gen Virol **89:**3047–3051. http://dx.doi.org/10.1099/vir.0.2008/002535-0.
23. **Pierson TC, Diamond MS.** 2012. Degrees of maturity: the complex structure and biology of flaviviruses. Curr Opin Virol **2:**168–175. http://dx.doi.org/10.1016/j.coviro.2012.02.011.
24. **Junjhon J, Edwards TJ, Utaipat U, Bowman VD, Holdaway HA, Zhang W, Keelapang P, Puttikhunt C, Perera R, Chipman PR, Kasinrerk W, Malasit P, Kuhn RJ, Sittisombut N.** 2010. Influence of pr-M cleavage on the heterogeneity of extracellular dengue virus particles. J Virol **84:**8353–8358. http://dx.doi.org/10.1128/JVI.00696-10.
25. **Pierson TC, Fremont DH, Kuhn RJ, Diamond MS.** 2008. Structural insights into the mechanisms of antibody-mediated neutralization of flavivirus infection: implications for vaccine development. Cell Host Microbe **4:**229–238. http://dx.doi.org/10.1016/j.chom.2008.08.004.
26. **Décembre E, Assil S, Hillaire MLB, Dejnirattisai W, Mongkolsapaya J, Screaton GR, Davidson AD, Dreux M.** 2014. Sensing of immature particles produced by dengue virus infected cells induces an antiviral response by plasmacytoid dendritic cells. PLoS Pathog **10:**e1004434. http://dx.doi.org/10.1371/journal.ppat.1004434.
27. **Nelson S, Jost CA, Xu Q, Ess J, Martin JE, Oliphant T, Whitehead SS, Durbin AP, Graham BS, Diamond MS, Pierson TC.** 2008. Maturation of West Nile virus modulates sensitivity to antibody-mediated neutralization. PLoS Pathog **4:**e1000060. http://dx.doi.org/10.1371/journal.ppat.1000060.
28. **Rodenhuis-Zybert IA, van der Schaar HM, da Silva Voorham JM, van der Ende-Metselaar H, Lei H-Y, Wilschut J, Smit JM.** 2010. Immature dengue virus: a veiled pathogen? PLoS Pathog **6:**e1000718. http://dx.doi.org/10.1371/journal.ppat.1000718.
29. **Colpitts TM, Rodenhuis-Zybert I, Moesker B, Wang P, Fikrig E, Smit JM.** 2011. prM-antibody renders immature West Nile virus infectious in vivo. J Gen Virol **92:**2281–2285. http://dx.doi.org/10.1099/vir.0.031427-0.
30. **Pryor MJ, Azzola L, Wright PJ, Davidson AD.** 2004. Histidine 39 in the dengue virus type 2 M protein has an important role in virus assembly. J Gen Virol **85:**3627–3636. http://dx.doi.org/10.1099/vir.0.80283-0.
31. **Hsieh S-C, Wu Y-C, Zou G, Nerurkar VR, Shi P-Y, Wang W-K.** 2014. Highly conserved residues in the helical domain of dengue virus type 1 precursor membrane protein are involved in assembly, precursor membrane (prM) protein cleavage, and entry. J Biol Chem **289:**33149–33160. http://dx.doi.org/10.1074/jbc.M114.610428.
32. **Hsieh S-C, Zou G, Tsai W-Y, Qing M, Chang G-J, Shi P-Y, Wang W-K.** 2011. The C-terminal helical domain of dengue virus precursor membrane protein is involved in virus assembly and entry. Virology **410:**170–180. http://dx.doi.org/10.1016/j.virol.2010.11.006.
33. **Peng J-G, Wu S-C.** 2014. Glutamic acid at residue 125 of the prM helix domain interacts with positively charged amino acids in E protein domain II for Japanese encephalitis virus-like-particle production. J Virol **88:**8386–8396. http://dx.doi.org/10.1128/JVI.00937-14.
34. **Lin Y-J, Wu S-C.** 2005. Histidine at residue 99 and the transmembrane region of the precursor membrane prM protein are important for the prM-E heterodimeric complex formation of Japanese encephalitis virus. J Virol **79:**8535–8544. http://dx.doi.org/10.1128/JVI.79.13.8535-8544.2005.
35. **Lin Y-J, Peng J-G, Wu S-C.** 2010. Characterization of the GXXXG motif in the first transmembrane segment of Japanese encephalitis virus precursor membrane (prM) protein. J Biomed Sci **17:**39. http://dx.doi.org/10.1186/1423-0127-17-39.
36. **Brault J-B, Kudelko M, Vidalain P-O, Tangy F, Desprès P, Pardigon N.** 2011. The interaction of flavivirus M protein with light chain Tctex-1 of human dynein plays a role in late stages of virus replication. Virology **417:**369–378. http://dx.doi.org/10.1016/j.virol.2011.06.022.
37. **Khadka S, Vangeloff AD, Zhang C, Siddavatam P, Heaton NS, Wang L, Sengupta R, Sahasrabudhe S, Randall G, Gribskov M, Kuhn RJ, Perera R, Lacount DJ.** 2011. A physical interaction network of dengue virus and human proteins. Mol Cell Proteomics **10:**M111.012187. http://dx.doi.org/10.1074/mcp.M111.012187.
38. **Mairiang D, Zhang H, Sodja A, Murali T, Suriyaphol P, Malasit P, Limjindaporn T, Finley RL.** 2013. Identification of new protein interactions between dengue fever virus and its hosts, human and mosquito. PLoS One **8:**e53535. http://dx.doi.org/10.1371/journal.pone.0053535.
39. **Kudelko M, Brault J-B, Kwok K, Li MY, Pardigon N, Peiris JSM, Bruzzone R, Desprès P, Nal B, Wang P-G.** 2012. Class II ADP-ribosylation factors are required for efficient secretion of dengue viruses. J Biol Chem **287:**767–777. http://dx.doi.org/10.1074/jbc.M111.270579.
40. **Duan X, Lu X, Li J, Liu Y.** 2008. Novel binding between pre-membrane protein and vacuolar ATPase is required for efficient dengue virus secretion. Biochem Biophys Res Commun **373:**319–324. http://dx.doi.org/10.1016/j.bbrc.2008.06.041.
41. **Gao F, Duan X, Lu X, Liu Y, Zheng L, Ding Z, Li J.** 2010. Novel binding between pre-membrane protein and claudin-1 is required for efficient dengue virus entry. Biochem Biophys Res Commun **391:**952–957. http://dx.doi.org/10.1016/j.bbrc.2009.11.172.
42. **Catteau A, Kalinina O, Wagner M-C, Deubel V, Courageot M-P, Desprès P.** 2003. Dengue virus M protein contains a proapoptotic sequence referred to as ApoptoM. J Gen Virol **84:**2781–2793. http://dx.doi.org/10.1099/vir.0.19163-0.
43. **Brabant M, Baux L, Casimir R, Briand JP, Chaloin O, Porceddu M, Buron N, Chauvier D, Lassalle M, Lecoeur H, Langonné A, Dupont S, Déas O, Brenner C, Rebouillat D, Muller S, Borgne-Sanchez A, Jacotot E.** 2009. A flavivirus protein M-derived peptide directly permeabilizes mitochondrial membranes, triggers cell death and reduces human tumor growth in nude mice. Apoptosis **14:**1190–1203. http://dx.doi.org/10.1007/s10495-009-0394-y.
44. **Hahn CS, Dalrymple JM, Strauss JH, Rice CM.** 1987. Comparison of the virulent Asibi strain of yellow fever virus with the 17D vaccine strain derived from it. Proc Natl Acad Sci U S A **84:**2019–2023. http://dx.doi.org/10.1073/pnas.84.7.2019.
45. **McElroy KL, Tsetsarkin KA, Vanlandingham DL, Higgs S.** 2006. Role of the yellow fever virus structural protein genes in viral dissemination from the Aedes aegypti mosquito midgut. J Gen Virol **87:**2993–3001. http://dx.doi.org/10.1099/vir.0.82023-0.
46. **Liang J-J, Liao C-L, Liao J-T, Lee Y-L, Lin Y-L.** 2009. A Japanese encephalitis virus vaccine candidate strain is attenuated by decreasing its interferon antagonistic ability. Vaccine **27:**2746–2754. http://dx.doi.org/10.1016/j.vaccine.2009.03.007.

47. **de Wispelaere M, Frenkiele MP, Despres P.** 2015. A Japanese encephalitis virus genotype 5 molecular clone is highly neuropathogenic in a mouse model: implication of the structural protein region in virulence. J Virol **89:**5862–5875. http://dx.doi.org/10.1128/JVI.00358-15.
48. **Pu S-Y, Wu R-H, Yang C-C, Jao T-M, Tsai M-H, Wang J-C, Lin H-M, Chao Y-S, Yueh A.** 2011. Successful propagation of flavivirus infectious cDNAs by a novel method to reduce the cryptic bacterial promoter activity of virus genomes. J Virol **85:**2927–2941. http://dx.doi.org/10.1128/JVI.01986-10.
49. **Mori Y, Okabayashi T, Yamashita T, Zhao Z, Wakita T, Yasui K, Hasebe F, Tadano M, Konishi E, Moriishi K, Matsuura Y.** 2005. Nuclear localization of Japanese encephalitis virus core protein enhances viral replication. J Virol **79:**3448–3458. http://dx.doi.org/10.1128/JVI.79.6.3448-3458.2005.
50. **Kim J-M, Yun S-I, Song B-H, Hahn Y-S, Lee C-H, Oh H-W, Lee Y-M.** 2008. A single N-linked glycosylation site in the Japanese encephalitis virus prM protein is critical for cell type-specific prM protein biogenesis, virus particle release, and pathogenicity in mice. J Virol **82:**7846–7862. http://dx.doi.org/10.1128/JVI.00789-08.
51. **Chien H-L, Liao C-L, Lin Y-L.** 2011. FUSE binding protein 1 interacts with untranslated regions of Japanese encephalitis virus RNA and negatively regulates viral replication. J Virol **85:**4698–4706. http://dx.doi.org/10.1128/JVI.01950-10.
52. **Katoh H, Mori Y, Kambara H, Abe T, Fukuhara T, Morita E, Moriishi K, Kamitani W, Matsuura Y.** 2011. Heterogeneous nuclear ribonucleoprotein A2 participates in the replication of Japanese encephalitis virus through an interaction with viral proteins and RNA. J Virol **85:**10976–10988. http://dx.doi.org/10.1128/JVI.00846-11.
53. **Schlesinger RW (ed).** 1980. The togaviruses: biology, structure, replication. Academic Press, New York, NY.
54. **Hunt AR, Cropp CB, Chang GJ.** 2001. A recombinant particulate antigen of Japanese encephalitis virus produced in stably-transformed cells is an effective noninfectious antigen and subunit immunogen. J Virol Methods **97:**133–149. http://dx.doi.org/10.1016/S0166-0934(01)00346-9.
55. **Zheng A, Umashankar M, Kielian M.** 2010. In vitro and in vivo studies identify important features of dengue virus pr-E protein interactions. PLoS Pathog **6:**e1001157. http://dx.doi.org/10.1371/journal.ppat.1001157.
56. **Yoshii K, Igarashi M, Ichii O, Yokozawa K, Ito K, Kariwa H, Takashima I.** 2012. A conserved region in the prM protein is a critical determinant in the assembly of flavivirus particles. J Gen Virol **93:**27–38. http://dx.doi.org/10.1099/vir.0.035964-0.
57. **Freeze HH, Kranz C.** 2008. Endoglycosidase and glycoamidase release of N-linked glycans. Curr Protoc Immunol Chapter 8:Unit 8.15. http://dx.doi.org/10.1002/0471142735.im0815s83.
58. **Mateo R, Nagamine CM, Spagnolo J, Méndez E, Rahe M, Gale M, Yuan J, Kirkegaard K.** 2013. Inhibition of cellular autophagy deranges dengue virion maturation. J Virol **87:**1312–1321. http://dx.doi.org/10.1128/JVI.02177-12.
59. **Zhang X, Sheng J, Plevka P, Kuhn RJ, Diamond MS, Rossmann MG.** 2013. Dengue structure differs at the temperatures of its human and mosquito hosts. Proc Natl Acad Sci U S A **110:**6795–6799. http://dx.doi.org/10.1073/pnas.1304300110.
60. **Zhang X, Sun L, Rossmann MG.** 2015. Temperature dependent conformational change of dengue virus. Curr Opin Virol **12:**109–112. http://dx.doi.org/10.1016/j.coviro.2015.04.006.
61. **Fibriansah G, Ng T-S, Kostyuchenko VA, Lee J, Lee S, Wang J, Lok S-M.** 2013. Structural changes of dengue virus when exposed to 37°C. J Virol **87:**7585–7592. http://dx.doi.org/10.1128/JVI.00757-13.
62. **Hung J-J, Hsieh M-T, Young M-J, Kao C-L, King C-C, Chang W.** 2004. An external loop region of domain III of dengue virus type 2 envelope protein is involved in serotype-specific binding to mosquito but not mammalian cells. J Virol **78:**378–388. http://dx.doi.org/10.1128/JVI.78.1.378-388.2004.
63. **Hanley KA, Manlucu LR, Gilmore LE, Blaney JE, Hanson CT, Murphy BR, Whitehead SS.** 2003. A trade-off in replication in mosquito versus mammalian systems conferred by a point mutation in the NS4B protein of dengue virus type 4. Virology **312:**222–232. http://dx.doi.org/10.1016/S0042-6822(03)00197-1.
64. **Villordo SM, Gamarnik AV.** 2013. Differential RNA sequence requirement for dengue virus replication in mosquito and mammalian cells. J Virol **87:**9365–9372. http://dx.doi.org/10.1128/JVI.00567-13.
65. **Smith KM, Nanda K, Spears CJ, Ribeiro M, Vancini R, Piper A, Thomas GS, Thomas ME, Brown DT, Hernandez R.** 2011. Structural mutants of dengue virus 2 transmembrane domains exhibit host-range phenotype. Virol J **8:**289. http://dx.doi.org/10.1186/1743-422X-8-289.
66. **Yoshii K, Yanagihara N, Ishizuka M, Sakai M, Kariwa H.** 2013. N-linked glycan in tick-borne encephalitis virus envelope protein affects viral secretion in mammalian cells, but not in tick cells. J Gen Virol **94:**2249–2258. http://dx.doi.org/10.1099/vir.0.055269-0.
67. **Senigl F, Grubhoffer L, Kopecky J.** 2006. Differences in maturation of tick-borne encephalitis virus in mammalian and tick cell line. Intervirology **49:**239–248. http://dx.doi.org/10.1159/000091471.
68. **Hase T, Summers PL, Eckels KH, Baze WB.** 1987. Maturation process of Japanese encephalitis virus in cultured mosquito cells in vitro and mouse brain cells in vivo. Arch Virol **96:**135–151. http://dx.doi.org/10.1007/BF01320956.
69. **Sreenivasan V, Ng KL, Ng ML.** 1993. Brefeldin A affects West Nile virus replication in Vero cells but not C6/36 cells. J Virol Methods **45:**1–17. http://dx.doi.org/10.1016/0166-0934(93)90135-E.
70. **Hase T, Summers PL, Eckels KH, Baze WB.** 1987. An electron and immunoelectron microscopic study of dengue-2 virus infection of cultured mosquito cells: maturation events. Arch Virol **92:**273–291. http://dx.doi.org/10.1007/BF01317484.
71. **Betts MJ, Russell RB.** 2007. Amino-acid properties and consequences of substitutions, p 311–342. *In* Barnes MR (ed), Bioinformatics for geneticists. John Wiley & Sons, Chichester, United Kingdom.
72. **Wang E, Ryman KD, Jennings AD, Wood DJ, Taffs F, Minor PD, Sanders PG, Barrett AD.** 1995. Comparison of the genomes of the wild-type French viscerotropic strain of yellow fever virus with its vaccine derivative French neurotropic vaccine. J Gen Virol **76:**2749–2755.
73. **Barrett ADT.** 1997. Yellow fever vaccines. Biologicals **25:**17–25. http://dx.doi.org/10.1006/biol.1997.0056.
74. **Guy B, Guirakhoo F, Barban V, Higgs S, Monath TP, Lang J.** 2010. Preclinical and clinical development of YFV 17D-based chimeric vaccines against dengue, West Nile and Japanese encephalitis viruses. Vaccine **28:**632–649. http://dx.doi.org/10.1016/j.vaccine.2009.09.098.
75. **Monath TP, Seligman SJ, Robertson JS, Guy B, Hayes EB, Condit RC, Excler JL, Mac LM, Carbery B, Chen RT, Brighton Collaboration Viral Vector Vaccines Safety Working Group (V3SWG).** 2015. Live virus vaccines based on a yellow fever vaccine backbone: standardized template with key considerations for a risk/benefit assessment. Vaccine **33:**62–72. http://dx.doi.org/10.1016/j.vaccine.2014.10.004.
76. **Lee E, Lobigs M.** 2008. E protein domain III determinants of yellow fever virus 17D vaccine strain enhance binding to glycosaminoglycans, impede virus spread, and attenuate virulence. J Virol **82:**6024–6033. http://dx.doi.org/10.1128/JVI.02509-07.
77. **Beck A, Tesh RB, Wood TG, Widen SG, Ryman KD, Barrett ADT.** 2014. Comparison of the live attenuated yellow fever vaccine 17D-204 strain to its virulent parental strain Asibi by deep sequencing. J Infect Dis **209:**334–344. http://dx.doi.org/10.1093/infdis/jit546.
78. **Ishikawa T, Yamanaka A, Konishi E.** 2014. A review of successful flavivirus vaccines and the problems with those flaviviruses for which vaccines are not yet available. Vaccine **32:**1326–1337. http://dx.doi.org/10.1016/j.vaccine.2014.01.040.
79. **Gao X, Li X, Li M, Fu S, Wang H, Lu Z, Cao Y, He Y, Zhu W, Zhang T, Gould EA, Liang G.** 2014. Vaccine strategies for the control and prevention of Japanese encephalitis in Mainland China, 1951-2011. PLoS Negl Trop Dis **8:**e3015. http://dx.doi.org/10.1371/journal.pntd.0003015.
80. **Yu Y.** 2010. Phenotypic and genotypic characteristics of Japanese encephalitis attenuated live vaccine virus SA14-14-2 and their stabilities. Vaccine **28:**3635–3641. http://dx.doi.org/10.1016/j.vaccine.2010.02.105.
81. **Zhao Z, Date T, Li Y, Kato T, Miyamoto M, Yasui K, Wakita T.** 2005. Characterization of the E-138 (Glu/Lys) mutation in Japanese encephalitis virus by using a stable, full-length, infectious cDNA clone. J Gen Virol **86:**2209–2220. http://dx.doi.org/10.1099/vir.0.80638-0.
82. **Yun S-I, Song B-H, Kim J-K, Yun G-N, Lee E-Y, Li L, Kuhn RJ, Rossmann MG, Morrey JD, Lee Y-M.** 2014. A molecularly cloned, live-attenuated japanese encephalitis vaccine SA14-14-2 virus: a conserved single amino acid in the ij hairpin of the viral E glycoprotein determines neurovirulence in mice. PLoS Pathog **10:**e1004290. http://dx.doi.org/10.1371/journal.ppat.1004290.
83. **Ye Q, Li X-F, Zhao H, Li S-H, Deng Y-Q, Cao R-Y, Song K-Y, Wang H-J, Hua R-H, Yu Y-X, Zhou X, Qin E-D, Qin C-F.** 2012. A single nucleotide mutation in NS2A of Japanese encephalitis-live vaccine virus

(SA14-14-2) ablates NS1′ formation and contributes to attenuation. J Gen Virol **93:**1959–1964. http://dx.doi.org/10.1099/vir.0.043844-0.

84. **Melian EB, Hinzman E, Nagasaki T, Firth AE, Wills NM, Nouwens AS, Blitvich BJ, Leung J, Funk A, Atkins JF, Hall R, Khromykh AA.** 2010. NS1′ of flaviviruses in the Japanese encephalitis virus serogroup is a product of ribosomal frameshifting and plays a role in viral neuroinvasiveness. J Virol **84:**1641–1647. http://dx.doi.org/10.1128/JVI.01979-09.
85. **Lauring AS, Jones JO, Andino R.** 2010. Rationalizing the development of live attenuated virus vaccines. Nat Biotechnol **28:**573–579. http://dx.doi.org/10.1038/nbt.1635.
86. **Larena M, Regner M, Lee E, Lobigs M.** 2011. Pivotal role of antibody and subsidiary contribution of CD8+ T cells to recovery from infection in a murine model of Japanese encephalitis. J Virol **85:**5446–5455. http://dx.doi.org/10.1128/JVI.02611-10.
87. **Prow NA, Setoh YX, Biron RM, Sester DP, Kim KS, Hobson-Peters J, Hall RA, Bielefeldt-Ohmann H.** 2014. The West Nile virus-like flavivirus Koutango is highly virulent in mice due to delayed viral clearance and the induction of a poor neutralizing antibody response. J Virol **88:**9947–9962. http://dx.doi.org/10.1128/JVI.01304-14.
88. **Kumar M, Roe K, Nerurkar PV, Namekar M, Orillo B, Verma S, Nerurkar VR.** 2012. Impaired virus clearance, compromised immune response and increased mortality in type 2 diabetic mice infected with West Nile virus. PLoS One **7:**e44682. http://dx.doi.org/10.1371/journal.pone.0044682.
89. **Wang K, Deubel V.** 2011. Mice with different susceptibility to Japanese encephalitis virus infection show selective neutralizing antibody response and myeloid cell infectivity. PLoS One **6:**e24744. http://dx.doi.org/10.1371/journal.pone.0024744.